Processing and Characterization of Multi-Walled Carbon Nanotubes Containing Alumina-Carbon Refractories Prepared by Nanocomposite Powder Technology

FENG LIANG, NAN LI, BAIKUAN LIU, and ZHONGYANG HE

Carbon nanotubes (CNTs) have often been used as additives to improve the properties of refractories containing carbon. However, it is very difficult to evenly distribute CNTs in the matrix. In order to solve this difficulty, an alumina/multi-walled carbon nanotube (MWCNT) (AM) composite powder in which MWCNTs had grown on the surfaces of Al_2O_3 particles was developed and used in alumina-carbon (Al_2O_3-C) refractories. The effects of the AM composite powders on the microstructure and properties of the Al_2O_3-C refractories were studied and compared with the commercial MWCNTs. The nanocomposite powders significantly improved the distribution uniformity of MWCNTs in the Al_2O_3-C matrix. The densification, fracture properties, thermal shock resistance, and slag corrosion resistance were enhanced due to the well-dispersed MWCNTs. On the contrary, no improvement of the densification, fracture properties, and thermal shock resistance of the refractories was achieved by addition of commercial MWCNTs due to the agglomeration of MWCNTs.

DOI: 10.1007/s11663-016-0647-4

I. INTRODUCTION

REFRACTORIES containing carbon are important materials used in the iron and steel industry. In recent years, nanoscale additives have been included in refractories containing carbon to improve their properties. For example, Roungos and Aneziris[1] reported that the combination of nanoscale powders based on carbon nanotubes (CNTs) and alumina nanosheets led to refractories with superior thermal shock performance and approximately 30 pct less residual carbon in comparison to commercially available Al_2O_3-C refractories. Bag *et al.*[2] added nanoscale carbon black into MgO-C refractories to reduce the carbon content and found that the mechanical properties, thermal shock resistance, and slag corrosion resistance were improved. Liu *et al.*[3] studied the effects of nanometer carbon black on the mechanical properties of low-carbon MgO-C refractories and found that the modulus of rupture and crushing strength increased gradually with increasing nanoscale carbon black content. Matsuo *et al.*[4] reported that the mechanical strength of MgO-C refractories was remarkably improved by the addition of carbon nanofibers. Pagliosa *et al.*[5] developed a special nanographite material to replace natural graphite flake and decrease the amount of carbon in MgO-Al_2O_3-C and MgO-C refractories. Luo *et al.*[6] reported that addition of 0.05 wt pct multi-walled carbon nanotubes (MWCNTs) into Al_2O_3-C refractories resulted in an increase of mechanical properties, whereas they got deteriorated with the further increase of MWCNTs amount from 0.1 to 1 wt pct.

However, in order to use nanoscale materials in refractories effectively, two key problems remain to be solved: First, a uniform distribution of the nanoscale materials in the matrix is required, and second, the price of the nanoscale materials must be reduced. Geol *et al.*[7] prepared an Al_2O_3 + graphite + nanocarbon composite by means of mechanical dispersion and surface functionalization, and the enhancement of thermal shock resistance of Al_2O_3-C refractories was obtained by adding this composite. Recent investigations had shown that when Al_2O_3-CNT composites were introduced into ceramics as starting materials, the mechanical properties and wear resistance of ceramic/CNT nanocomposites could be improved to some extent.[8–11]

Up to now, the Al_2O_3-CNT composites had prepared using various mixing methods, but it was difficult to obtain a highly uniform distribution of CNTs in the composites. In this study, a novel method of preparing MWCNTs containing Al_2O_3-C refractories had been developed by introducing Al_2O_3/MWCNT (AM) composite powders in which MWCNTs had grown on the surfaces of Al_2O_3 particles. When the nanocomposite powders were used as the CNT source, the distribution of MWCNTs in the refractory matrix should be greatly improved. In the present study, the effect of increasing

FENG LIANG, Postdoctoral Researcher, and NAN LI, Professor, are with The State Key Laboratory of Refractories and Metallurgy, Wuhan University of Science and Technology, Wuhan 430081, China. Contact e-mail: liangfengref@wust.edu.cn BAIKUAN LIU, Chief Executive Officer, and ZHONGYANG HE, Chief Research Officer, are with Puyang Refractories Group Co., Ltd., Puyang 457100, China.
Manuscript submitted May 27, 2015.
Article published online March 25, 2016.

amount of MWCNTs on the properties of Al_2O_3-C refractories prepared by nanocomposite powder technology was studied. Composition with the same MWCNT content was also compared with conventional processing by mixing with commercial MWCNTs under exactly similar conditions.

II. EXPERIMENTAL PROCEDURE

A. *Preparation of Al_2O_3/MWCNT Composite Powders*

The preparation of Al_2O_3/MWCNT composite powders was carried out at atmospheric pressure *via* catalytic decomposition of methane in a stainless-steel fixed-bed reactor (length and diameter of the reactor were 500 and 300 mm, respectively) using Fe-Ni/Al_2O_3 catalysts. The catalysts were prepared by conventional impregnation method with total metals loading adjusted to 0.2 wt pct. $Fe(NO_3)_3{\cdot}9H_2O$ and $Ni(NO_3)_2{\cdot}6H_2O$ (supplied by Aldrich) were used as metal sources, and tabular alumina particles (<43 μm, supplied by Almatis) were used as the catalyst support. The Fe:Ni molar ratio was 1:1. The catalyst and MWCNT preparation procedures have been described previously.[12,13] Two AM composite powders with different carbon contents of 0.52 and 0.98 wt pct were prepared by adjusting the methane flow rate. The carbons deposited on the catalyst were analyzed using scanning electron microscope (SEM, Nova 400 NanoSEM, FEI Company, USA) and high-resolution transmission electron microscope (HRTEM, 2000F, Jeol Ltd., Japan).

B. *Preparation of Al_2O_3-C Refractory Samples*

White fused alumina (98.51 pct Al_2O_3, Zhengzhou Zhongtian Special Alumina Co., Ltd., China) in two different size classes (3 to 1 and <1 mm), tabular alumina powder (<0.043 mm, 99.42 pct Al_2O_3, Qingdao Almatis Co., Ltd., China), silicon powder (<0.074 mm, 98.45 pct Si, Anyang Yuhong Metallurgy & Refractory Co., Ltd., China), and graphite flake (<0.147 mm, 97.52 pct fixed carbon, Qingdao Tianhe Graphite Co., Ltd., China) were used as the raw materials. Thermosetting phenolic resin (liquid, 40 pct fixed carbon, Wuhan Lifa Chemistry & Industry Co., Ltd., China) was added as a binder.

The as-prepared AM composite powders and commercial MWCNTs (purity >98 pct, Alpha Nano Tech. Inc., Chengdu, China) were used as CNT sources, respectively. The SEM and TEM images of various CNT sources are shown in Figure 1. These images show that MWCNTs with diameters of 10-50 nm had formed on the surfaces of the Al_2O_3 particles in the nanocomposite powders (Figures 1(a) through (c)). The commercial MWCNTs are bulk aggregates in which MWCNTs with diameters of 20-70 nm were typically curved and twisted (Figures 1(d) and (e)). These aggregates were very difficult to disperse.

The batch compositions of the Al_2O_3-C refractory samples are given in Table I. There were no MWCNTs in sample C0. The MWCNTs in samples C1 and C2 were introduced by AM composite powders, while the MWCNTs in sample CT were introduced as commercial MWCNTs. The raw materials were mixed and bound

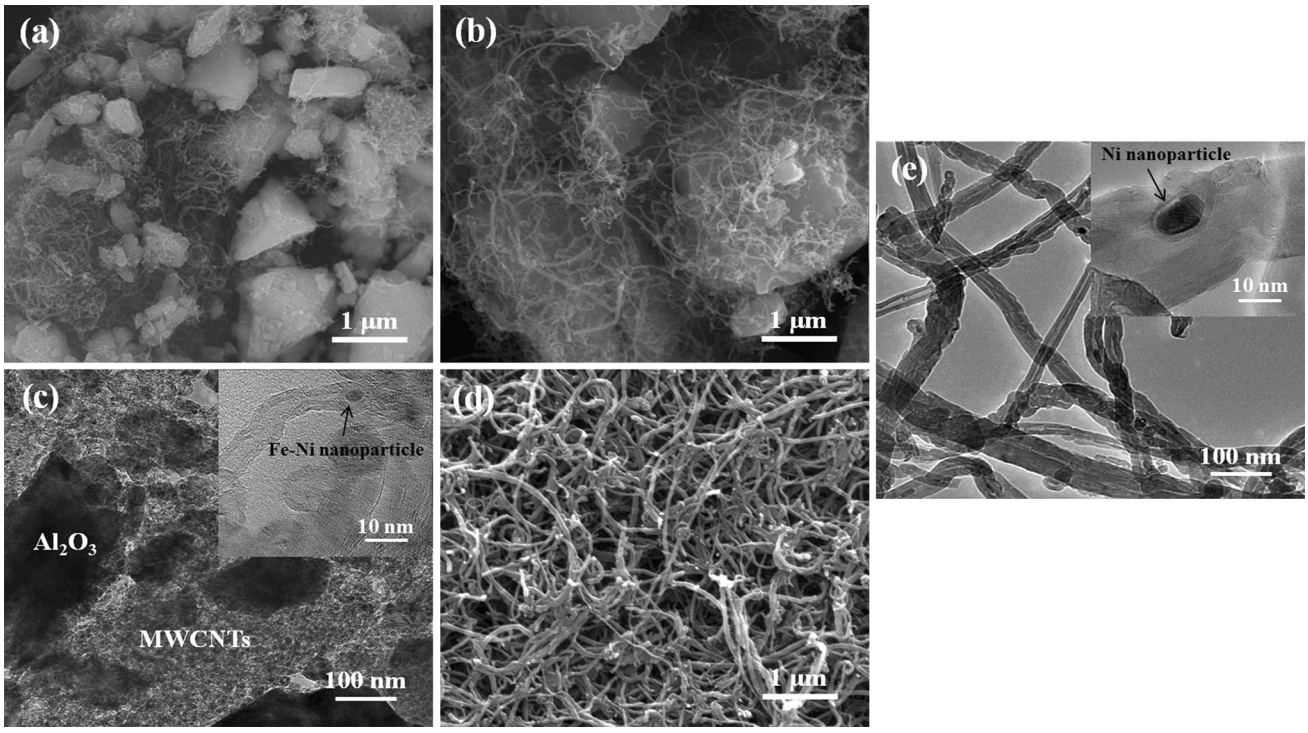

Fig. 1—SEM and HRTEM micrographs of Al_2O_3/MWCNT composite powders with different CNT contents and commercial MWCNTs: (*a*) SEM image of the nanocomposite powders containing 0.52 pct MWCNT, (*b*) SEM image of the nanocomposite powders containing 0.98 pct MWCNTs, (*c*) HRTEM images of the nanocomposite powders; (*d*) SEM images of commercial MWCNTs, (*e*) HRTEM images of the commercial MWCNTs. Insets show the high-magnification images.

Table I. Formulations of Al_2O_3-C Refractory Samples (Weight Percent)

Ingredient	Sample Code			
	C0	C1	C2	CT
White Fused Alumina (3 to 0 mm)	65	65	65	65
Al_2O_3/MWCNT Composite Powders		30	30	
Tabular Alumina	30			29.7
Silicon Powder	2	2	2	2
Graphite Flakes	3	3	3	3
MWCNTs	0	(0.15)	(0.3)	0.3
Phenolic Resin (Liquid)	+4	+4	+4	+4

Parentheses denote MWCNTs from AM composite powders.

with phenolic resin and then aged at room temperature for 36 hours. Bar samples of dimension 25 mm × 25 mm × 140 mm and crucible samples (height = 50 mm, diameter = 50 mm) with a hole of dimension 20 mm diameter and 18 mm height were prepared by pressing under a pressure of 150 MPa and then cured at 493 K (220 °C) for 24 hours. Finally, the as-prepared samples were fired at 1273 K and 1673 K (1000 °C and 1400 °C) in a saggar filled with fine petroleum coke powders.

C. *Tests and Characterization Methods*

The apparent porosity (AP) and bulk density (BD) of the samples were measured according to Archimedes' principle with water as medium. The fracture properties of the bar samples, including flexural strength σ, Young's modulus E, and work of fracture γ_{WOF}, were measured by the three-point bending test at ambient temperature with a span of 100 mm and a loading rate of 0.5 mm/min using an electronic digital control system (EDC 120, DOLI Company, Germany), where γ_{WOF} was determined by the single-edge-notch-beam method (SENB) using notched bars with notches of 1 mm in width and 6 mm in depth.

The theoretical thermal shock parameter R^{IV}[14] was then calculated in order to predict thermal shock behavior of the samples as follows:

$$R^{IV} = \frac{E\gamma_{WOF}}{\sigma^2(1-v)}, \quad [1]$$

where v is the Poisson ratio, measured by resonant frequency and damping analyzer (RFDA, HTVP 1600, IMCE, Belgium) in accordance with ASTM E 1876-1999.

The thermal shock resistance test was carried out *via* heating–cooling process. The samples fired at 1273 K (1000 °C) were heated in a coke bed up to 1373 K (1100 °C) with a heating rate of 5 K/min and then soaked at this temperature for 30 minutes. Then, the samples were taken out and quickly quenched into a large container of silicone oil at room temperature. This cycle was repeated for 3 times. The residual flexural strength was measured, and the thermal shock resistance was evaluated as the residual strength ratio of flexural strength, i.e., σ_f/σ_{f0} ratio, where σ_{f0} is the flexural strength of the original sample and σ_f is the flexural strength of the quenched sample. Slag corrosion test by static crucible method was done for all the different samples using the cured crucibles as shown in Figure 2(a), at 1773 K (1500 °C) for 3 hours in a reducing atmosphere using steel converter slag (composition given in Table II). The corroded samples were cut horizontally into two pieces, and the original and the corroded (as pointed out by the shaded area in Figure 2(b)) areas of the sample cross section were measured, namely S_0 and S. After that, the corrosion index $I = S/S_0 \times 100$ pct was evaluated.

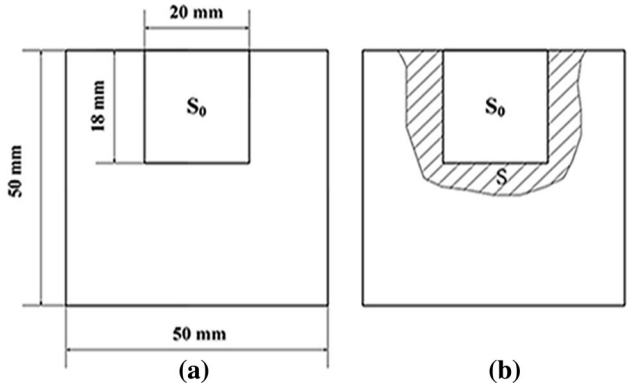

Fig. 2—Sketch of the crucible for the slag corrosion resistance test. S_0 is the area of the hole in the original crucible, and S is the corroded area of the crucible after testing.

The phase compositions of the fired samples were analyzed by X-ray diffraction (XRD, X'Pert Pro, Philips, Netherlands). The microstructures of ruptured surfaces of all the fired samples were observed by SEM, equipped with energy-dispersive X-ray spectroscope (EDS, Noran 623M-3SUT, Thermo Electron Corporation, Japan).

III. RESULTS

A. *Phase Compositions*

In order to observe the effect of MWCNTs addition and temperature on the phase compositions, XRD patterns of samples fired at 1273 K and 1673 K (1000 °C and 1400 °C) are measured and shown in

Table II. Chemical Composition of Slag (Weight Percent)

SiO_2	Al_2O_3	Fe_2O_3	CaO	MgO	K_2O	Na_2O	TiO_2
12.18	2.10	31.01	41.59	9.30	0.035	0.05	0.66

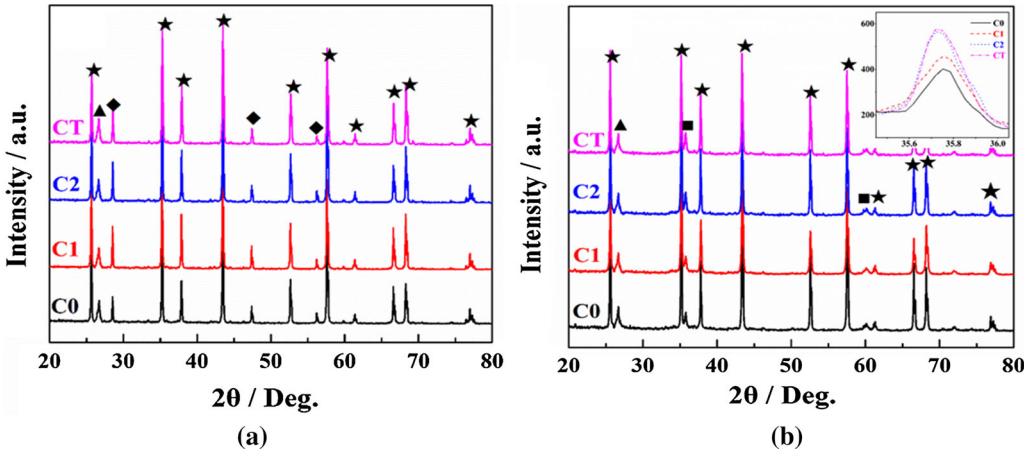

Fig. 3—XRD patterns of samples fired at different temperatures: (*a*) 1273 K (1000 °C) and (*b*) 1673 K (1400 °C). ★: Corundum, ■: *β*-SiC, ◆: Si, ▲: Graphite. Inset shows *β*-SiC (111) planes of samples.

Figure 3. Al_2O_3, Si, and graphite flake phases were detected after fired at 1273 K (1000 °C) (Figure 3(a), indicating that no new ceramic phases formed at this temperature. With further increasing the firing temperature to 1673 K (1400 °C), SiC phase formed, while the peak intensity of Si phase disappeared completely (Fig. 3(b)). The peak intensity of SiC phase increased with the increase of MWCNT content (inset in Figure 3(b)), and the peak intensity of SiC phase was similar for sample C2 and CT with the same MWCNT content, that is to say, the amount of ceramic phases SiC was increased by the addition of MWCNTs. SiC were synthesized by reacting graphite flake and MWCNTs with Si particles, while MWCNTs acted as additional carbon source.[15,16]

B. *Microstructure*

Figures 4 and 5 show SEM micrographs of samples C0, C2, and CT treated at 1273 K and 1673 K (1000 °C and 1400 °C) for 3 h, respectively. Among the samples treated at 1273 K (1000 °C), sample C0 shown some graphite particles in its SEM image (Figure 4(a)), whereas MWCNTs were found on the surfaces of the Al_2O_3 particles in sample C2 (Figure 4(b)). For sample CT, the MWCNT was aggregated (Figure 4(c)). After fired at 1673 K (1400 °C), some SiC whiskers formed in sample C0 as a result of the reaction between graphite and silicon. Many uniformly distributed SiC whiskers formed through the reaction between silicon and MWCNTs or graphite were observed in sample C2 (Figure 5(b)). Moreover, SiC whiskers were also observed in sample CT (Figure 5(c)), but most of them were just on the surfaces of MWCNT aggregates. It was obvious that the uniformity of the MWCNT distribution in the matrix of the Al_2O_3-C refractories was remarkably improved when the AM powders were used as the MWCNT source.

C. *Apparent Porosity and Bulk Density*

The change in apparent porosity and bulk density at various temperatures is shown in Table III. For the samples C1 and C2, prepared using Al_2O_3/MWCNT composite powders, increasing MWCNT content reduced the AP value and raised the BD value. This is due to increased filling of the inter-particle spaces of the refractory by much finer nano-sized materials. However, the reduction in density was obtained in sample CT with the addition of commercial MWCNTs. CNT aggregates would reduce the density of the composite because of their porous rope-like structure.[17] The decreases of the density in the sample CT indicated that many CNT aggregates remain in the matrix, as shown in Figure 4(c). Kim *et al.*[18] reported that well-dispersed CNTs in a matrix lead to higher densities, while agglomerates result in lower densities. In this context, the sample C1 and C2 had higher densities. It could be confirmed that successful dispersion of MWCNTs within the Al_2O_3-C matrix should be obtained using AM composite powders, corresponding with the observed microstructure (Figure 4(b)).

In addition, it is obvious that the apparent porosity increased with increasing the firing to 1273 K (1000 °C), but it decreased dramatically at 1673 K (1400 °C); correspondingly, the change in bulk density as a function of firing temperature was opposite to apparent porosity. The higher apparent porosity at 1273 K (1000 °C) was due to the release of volatile species of the binder. The reduction of apparent porosity at 1673 K (1400 °C) was considered as a direct consequence of formation of SiC phases in the materials.

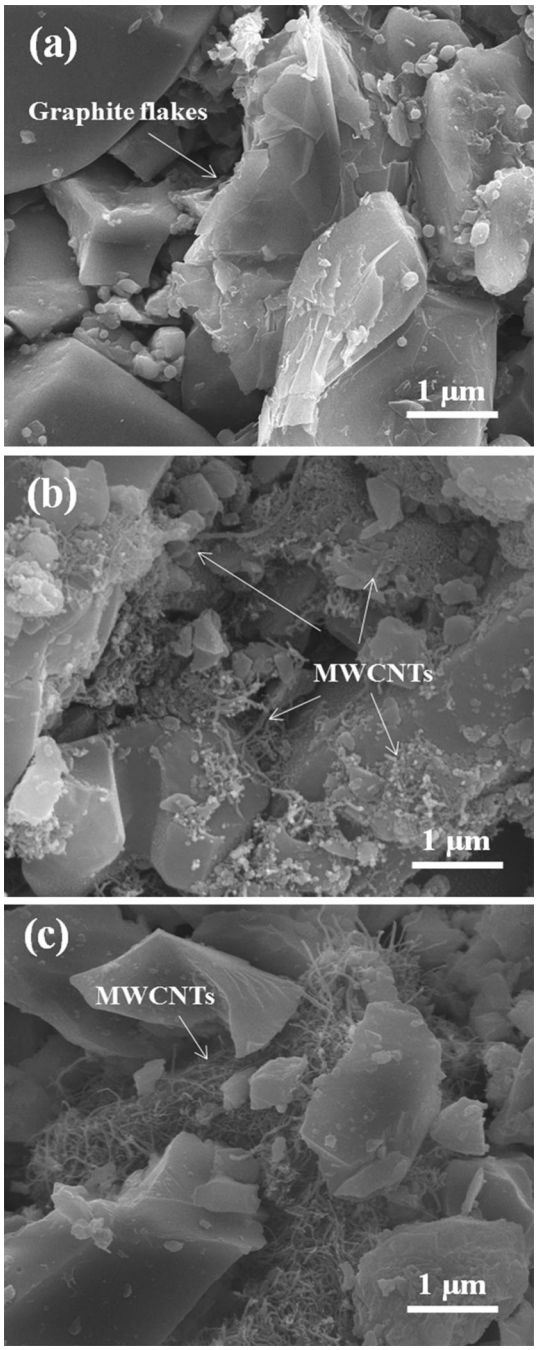

Fig. 4—SEM micrographs of samples (*a*) C0, (*b*) C2, (*c*) CT fired at 1273 K (1000 °C) for 3 h.

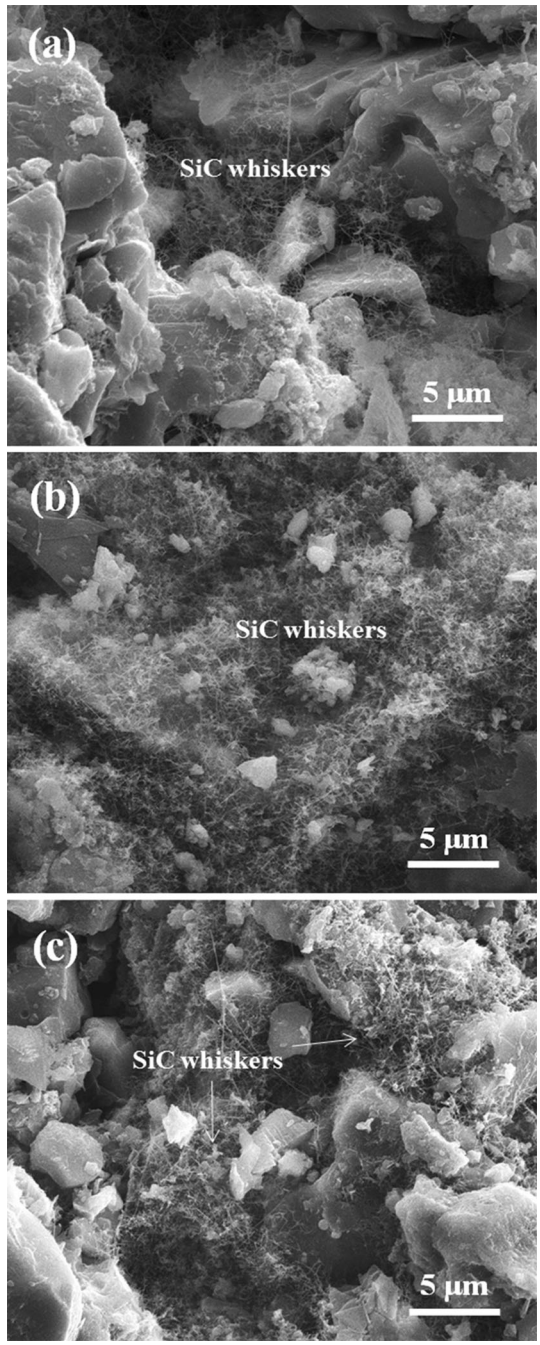

Fig. 5—SEM micrographs of samples (*a*) C0, (*b*) C2, (*c*) CT fired at 1673 K (1400 °C) for 3 h.

Moreover, more SiC whiskers were formed by the addition of MWCNTs and its homogeneous distribution in the matrix, resulting in a lower porosity of samples containing AM composite powders.

D. *Fracture Properties and Thermal Shock Resistance*

Table IV shows the testing results of fracture properties and calculated thermal shock resistance parameters of samples fired at 1273 K (1000 °C). For the samples prepared using AM composite powders, with the increase of MWCNT content, the flexural strength increased continuously. The flexural strength of sample C2 was improved 23.5 pct. With the increase of MWCNT content, better filling as well as better compaction had occurred, resulting in a better strength. There was also similar improvement observed in the elastic modulus of samples, indicating that slow crack propagation occurred. The work of fracture γ_{WOF} of sample C2 confirmed that ~50 pct more energy was required for crack propagation compared to C0. Due to the lower density, the fracture properties decreased in sample CT containing MWCNT aggregates on the contrary. This phenomenon was also found in carbon

Table III. AP and BD of Samples After Heat Treatment at Various Temperatures

	493 K (220 °C)		1273 K (1000 °C)		1673 K (1400 °C)	
Sample Code	AP (Pct)	BD (g/cm^3)	AP (Pct)	BD (g/cm^3)	AP (Pct)	BD (g/cm^3)
C0	14.5	3.08	17.2	3.03	16.5	3.05
C1	13.8	3.14	15.2	3.06	14.2	3.10
C2	13.0	3.17	14.3	3.10	13.6	3.15
CT	15.1	3.05	18.5	3.00	17.5	3.02

Table IV. Fracture Properties and Thermal Shock Resistance Parameters of Samples Fired at 1273 K (1000 °C)

Specimen code	C0	C1	C2	CT
σ_{f0} (MPa)	5.5	6.2	7.1	4.8
E (GPa)	4.5	5.3	5.9	3.6
γ_{WOF} (J/m^2)	18.8	25.6	36.4	15.2
R^{IV} ($\times 10^{-6}$ m)	3.5	3.9	4.6	3.2

nanotube/alumina composites.[19–21] Furthermore, as predicted from R^{IV} parameter, indicating the minimum in the elastic energy at fracture available for crack propagation,[22] sample C2 appeared to have higher resistance to fracture propagation caused by the thermal stresses in consequence of the presence of well-dispersed MWCNTs.

After thermal shock parameters were calculated, the behavior of materials was predicted on that basis. These predictions were compared with the experimental thermal shock test data (Figure 6). All the samples containing AM composite powders exhibited higher residual strength compared to C0 without MWCNTs and CT with MWCNT aggregates. The sample C2 with 0.3 wt pct MWCNTs added had the highest residual strength ratio of 0.76, but 0.37 for C0 and 0.35 for CT, indicating that the addition of MWCNTs with homogeneous distribution was favorable to improve the thermal shock resistance of Al_2O_3-C refractories.

E. *Slag Corrosion Resistance*

The corrosion indexes of the refractory without and with MWCNTs are shown in Figure 7. Incorporation of MWCNTs was observed to significantly inhibit the slag corrosion. The nanocarbon prevents the corrosion of the matrix by forming a coating of carbon on the surface due to its high surface to volume ratio.[23] Hence, addition of nanocarbon in Al_2O_3-C refractory exhibits better slag corrosion resistance, as also observed by Bag *et al.*[2] Increase in MWCNTs greatly decreased the corrosion index. Higher amount of MWCNTs increased its distribution throughout the matrix and reduced the slag corrosion. There was a significant rise in the corrosion index of sample CT, compared to that of sample C2 with the same MWCNT content. It may be suggested that MWCNT aggregates was less effective for the improvement of slag corrosion resistance than AM composite powders.

IV. DISCUSSION

As mentioned above, the addition of AM composite powders improved the properties of Al_2O_3-C refractories because of the increased uniformity of MWCNTs in the matrixes. For example, in sample C2, the MWCNTs existed at the surfaces of Al_2O_3 particles and were evenly distributed in the matrix, and these MWCNTs could be dispersed evenly among the tiny spaces between coarse, medium, and fine particles, thereby filling in the pores and gaps (Figure 4(b)) to reduce the porosity and enhance the density, resulting in the observed improvement of fracture properties of Al_2O_3-C refractory. In previous studies,[24–26] obtaining high densities had been deemed important for producing composite ceramics with excellent mechanical and fracture properties. In addition, MWCNTs with strengthening and toughening mechanisms, including crack deflection, bridging, fracture, and pull-out, strengthened the samples, leading to the better mechanical and fracture properties.[27] Meanwhile, the homogeneously dispersed MWCNTs not only absorbed and relieved thermal stresses but also reduced any maldistribution of thermal stresses in the interiors of the refractories, thus improving the thermal shock resistance.[2,23]

Comparing against sample C2, there was a significant rise in the apparent porosity of sample CT prepared using commercial MWCNTs with the same MWCNT content. The MWCNTs existed as aggregates in the matrix, as shown in Fig. 4(c), and severe phase segregation was presented in the microstructure, giving MWCNT aggregates a similar role to pores in the matrix, as reported and explained by Gallardo-López *et al.*[28] On other hand, bundles of CNTs likely acted as flaws and resulted in the lower observed properties,[21] so that poor dispersion of MWCNTs (agglomeration) could cancel out the advantages of MWCNTs. The property tests have shown that no improvement of the densification, fracture properties, and thermal shock

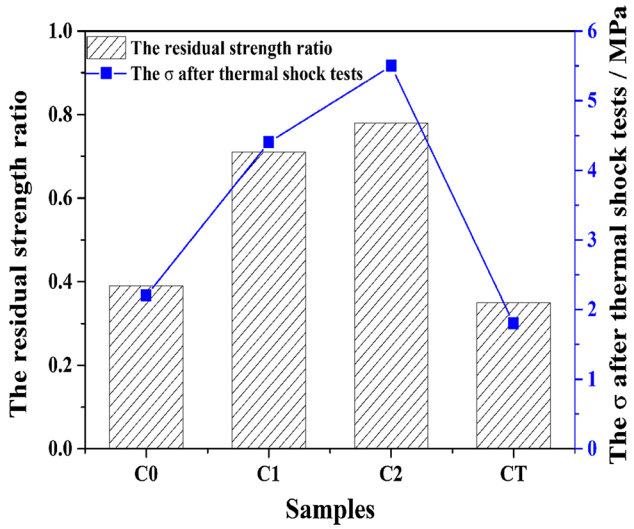

Fig. 6—The residual flexural strength and the residual strength ratio of the samples after 3 thermal shocks.

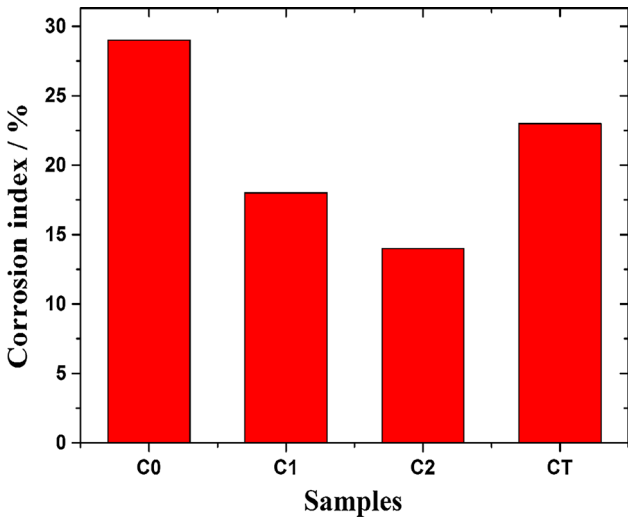

Fig. 7—Corrosion indexes of samples after slag corrosion resistance test.

resistance of the refractories was achieved by addition of commercial MWCNTs.

Furthermore, the results of the slag corrosion test at 1773 K (1500 °C) (Figure 7) show that increase in MWCNTs greatly improved the slag corrosion resistance of the refractories prepared using AM composite powders; however, the slag corrosion resistance of sample CT was lower than that of sample C2 with the same MWCNT content. The results were attributed to two reasons. First, as shown in Table III, well-dispersed MWCNTs reduced the apparent porosity of Al_2O_3-C refractories, while MWCNT agglomerates result in higher porosity. Moreover, more SiC whiskers were formed at 1673 K (1400 °C) and homogeneously distributed in the samples containing AM composite powders (Figure 5(b)), resulting in a higher density. The low porosity and high density of refractories contributed to the slag corrosion resistance, as reported by Campos *et al.*[29] and Braulio *et al.*[30] Second, the non-wetting behavior of molten slag on SiC and MWCNTs impeded the penetration of slag and enhanced the slag corrosion resistance of the refractories.[31,32]

V. CONCLUSIONS

Compared with the addition of the commercial MWCNTs by means of mixing, the addition of Al_2O_3/MWCNT composite powders in which MWCNTs had grown on the surfaces of Al_2O_3 particles substantially improved the distribution uniformity of MWCNT in the Al_2O_3-C matrix, thereby filling in a better way among the spaces between particles of starting materials and filling of interior pores and gaps. This consequently enhanced the properties of the Al_2O_3-C refractories, such as the densification, fracture properties, thermal shock resistance, and slag corrosion resistance. At the elevated temperature, the MWCNTs on the surfaces of the Al_2O_3 grains reacted with Si to form SiC whiskers, resulting in further increases in density and improvements of the other properties. On the contrary, no improvement of the densification, fracture properties, and thermal shock resistance of the refractories was achieved by addition of the commercial MWCNTs due to the agglomeration of MWCNTs. Such nanocomposite powders should also be used in other refractories containing carbon and CNT composites, leading to significant advances in refractory materials for the iron and steel industry.

ACKNOWLEDGMENTS

This work was supported by the China Postdoctoral Science Foundation (2014M560631), National Natural Science Foundation of China (General program, 51502216, 51472184, 51472185), and State Basic Research Development Program of China (973 Program, 2014CB660802), and the authors also wish to express their gratitude to Puyang Refractories Co., Ltd., for the financial support rendered to this work.

REFERENCES

1. V. Roungos and C.G. Aneziris: *Ceram. Int.*, 2012, vol. 38, pp. 919–27.
2. M. Bag, S. Adak, and R. Sarkar: *Ceram. Int.*, 2012, vol. 38, pp. 2339–46.
3. B. Liu, J.L. Sun, G.S. Tang, K.Q. Liu, L. Li, and Y.F. Liu: *J. Iron. Steel. Res.*, 2010, vol. 17, pp. 75–78.
4. Y. Matsuo, M. Tanaka, J. Yoshitomi, S.H. Yoon and J. Miyawaki: 'Effect of the carbon nanofiber addition on the mechanical properties of MgO-C brick', in 12th Unified International Technical Congress on Refractories, Kyoto, Japan, 2011, 2-E-13.
5. C. Pagliosa, L.R. Bittencourt, P.O. Brant, A. Campos and N. Freire: 'Magnesia-Alumina-Carbon (MAC) bricks for steel ladle metal line and MgO-C for BOF: Integral solution with

nanotechnology', in 12th Unified International Technical Congress on Refractories, Kyoto, Japan, 2011, 2-E-12.
6. M. Luo, Y. Li, S. Jin, S. Sang, L. Zhao, and Y. Li: *Mater. Sci. Eng. A*, 2012, vol. 548, pp. 134–41.
7. B.J. Geol, C.D. Moon and N.Y. Han: 'The effect of applying nano carbon in carbon containing refractories', in 12th Unified International Technical Congress on Refractories, Kyoto, Japan, 2011, 2-E-14.
8. S.C. Zhang, W.G. Fahrenholtz, G.E. Hilmas, and E.J. Yadlowsky: *J. Eur. Ceram. Soc*., 2010, vol. 30, pp. 1373–80.
9. S. Bi, G.L. Hou, X.J. Su, Y.D. Zhang, and F. Guo: *Mater. Sci. Eng. A*, 2011, vol. 528, pp. 1596–1601.
10. V. Puchy, P. Hvizdos, and J.F. Dusza: Kovac, F. Inam and M.J. Reece*Ceram. Int*., 2013, vol. 39, pp. 5821–26.
11. A. Kasperski, A. Weibel, C. Estournès, C. Laurent, and A. Peigney: *Scripta Mater*., 2014, vol. 75, pp. 46–49.
12. S.P. Chai, S.H.S. Zein, and A.R. Mohamed: *Appl. Catal. A*, 2007, vol. 326, pp. 173–79.
13. J.L. Song, L. Wang, S.A. Feng, J.H. Zhao, and Z.P. Zhu: *New Carbon Mater*., 2009, vol. 24, pp. 307–13.
14. D.P.H. Hasselman: *J. Am. Ceram. Soc*., 1969, vol. 52, pp. 600–604.
15. W. Xei, G. Möbus, and S. Zhang: *J. Mater. Chem*., 2011, vol. 21, pp. 18325–30.
16. K.P. So, J.C. Jeong, J.G. Park, H.K. Park, Y.H. Choi, D.H. Noh, D.H. Keum, H.Y. Jeong, C. Biswas, C.H. Hong, and Y.H. Lee: *Compos. Sci. Technol*., 2013, vol. 74, pp. 6–13.
17. A.G. Rinzler, J. Liu, H. Dai, P. Nikolaev, C.B. Huffman, F.J. RodriguezMacias, P.J. Boul, A.H. Lu, D. Heymann, D.T. Colbert, R.S. Lee, J.E. Fischer, A.M. Rao, P.C. Eklund, and R.E. Smalley: *Appl. Phys. A*, 1998, vol. 67, pp. 29–37.
18. B.N. Kim, S. Wakayama, and M. Kawahara: *Int. J. Fract*., 1996, vol. 75, pp. 247–59.
19. J. Cho, A.R. Boccaccini, and M.S.P. Shaffer: *J. Mater. Sci*., 2009, vol. 44, pp. 1934–51.
20. R.H. Woodman, B.R. Klotz, and R.J. Dowding: *Ceram. Int*., 2005, vol. 31, pp. 765–68.
21. G Yamamoto, M Omori, K Yokomizo, T Hashida, and K Adachi: *Mater. Sci. Eng. B*, 2008, vol. 148, pp. 265–69.
22. N. Rendtorffa and E. Aglietti: *Mater. Sci. Eng., A*, 2010, vol. 527, pp. 3840–47.
23. T. Ochiai: *J. Tech. Assoc. Refract. Jpn*, 2005, vol. 25, pp. 4–11.
24. A. Mukhopadhyay, B.T.T. Chu, M.L.H. Green, and R.I. Todd: *Acta Mater*., 2010, vol. 58, pp. 2685–97.
25. A. Peigney, F.L. Garcia, C. Estournès, A. Weibel, and C. Laurent: *Carbon*, 2010, vol. 48, pp. 1952–60.
26. I. Ahmad, H. Cao, H. Chen, H. Zhao, A. Kennedy, and Y.Q. Zhu: *J. Eur. Ceram. Soc*., 2010, vol. 30, pp. 865–73.
27. S.K. Singhal, R. Pasricha, M. Jangra, R. Chahal, S. Teotia, and R.B. Mathu: *Powder Technol*., 2012, vol. 215, pp. 254–63.
28. A. Gallardo-López, R. Poyato, A. Morales-Rodríguez, A. Fernández-Serrano, A. Muñoz, and A. Domínguez-Rodríguez: *J. Mater. Sci*., 2014, vol. 49, pp. 7116–23.
29. K.S. Campos, G.F.B.L. Silva, E.H.M. Nunes, and W.L. Vasconcelos: *Ceram. Int*., 2012, vol. 38, pp. 5661–67.
30. MAL Braulioa, AG Tombamartinez, AP Luz, C Liebske, and VC Pandolfelli: *Ceram. Int*., 2011, vol. 37, pp. 1935–45.
31. S.H. Heo, K. Lee, and Y. Chung: *T. Nonferr. Metal. Soc*., 2012, vol. 22, pp. 870–75.
32. D.X. Yang, Y.G. Liu, M.H. Fang, Z.H. Huang, and D.Y. Ye: *Ceram. Int*., 2014, vol. 40, pp. 1593–98.